# **Polymers**



# Deformation of microfibrillated chitin film and composites

Michael Ikpi Ofem<sup>1,\*</sup>

<sup>1</sup> Department of Mechanical Engineering, Cross River University of Technology, Calabar, Nigeria

Received: 26 October 2017 Accepted: 23 February 2018

© Springer Science+Business Media, LLC, part of Springer Nature 2018

# **ABSTRACT**

Composites of poly(acrylic acid) (PAA) and chitin whiskers were prepared using evaporation method. The weight fraction of chitin whiskers (CHW) was varied from 73 to 23%. Raman was utilised for the first time to monitor the deformation of chitin film and chitin-reinforced PAA composites. The Raman band located at 1622 cm $^{-1}$  was monitored for deformation. On application of tensile force, the Raman band initially found at 1622 cm $^{-1}$  corresponding to the single H-bonded amide one spectrum shifted towards a lower wavenumber. Raman band shift rates of  $-1.85 \text{ cm}^{-1}/\%$  for chitin film and -0.25, -0.59 and  $-0.59 \text{ cm}^{-1}/\%$  for 23, 43 and 73 wt% CHW whiskers, respectively, were obtained. The Young modulus of composites materials and whiskers were 37, 16 and 115 GPa, respectively, for a two-dimensional in-plane distribution of CHW. CHW within PAA did not show any preferential alignment. At high volume or weight of PAA or low weight CHW (3, 11% chitin) monitoring of the Raman peak shift was difficult.

## Introduction

With the advent of Raman spectroscopy, its application cut across a broad field and has been used in pharmaceutical research and development. Raman spectroscopy has also found its application in shelf-life assessment, drug formula and in non-invasive analysis in pharmacokinetic analysis [1–3]. It has been used to differentiate polymorphs of chitin [4, 5]. Raman spectroscopy can be used to monitor stress transfer between cellulose whiskers and polymer matrices. Studies on the deformations of cellulose whiskers, wood and paper with the aid of Raman spectroscopy have been extensively reported, with

focus on the Raman band initially located at  $1095~\rm cm^{-1}$ . This band corresponds to the C–O ring stretching mode within the cellulose backbone. Six different regenerated cellulose fibres, wood and paper were studied for mechanical deformation [6]. The Raman band peak at  $1095~\rm cm^{-1}$  for all the regenerated cellulose fibres shifted linearly towards a lower wavenumber. The stress values of the fibres cluster within a small range gave stress sensitivity value of  $-4.5\pm0.1~\rm cm^{-1}/GPa$ , while the strain values were found to vary. Paper deformation shows three stages of deformation before failure. These are the linear, nonlinear and the debonding deformation stages. The cellulose fibres of Pinewood were acting

Address correspondence to E-mail: ofemic@yahoo.com

🙆 Springer

as reinforcement. The peak at 1095 cm<sup>-1</sup> shifted to a lower wavenumber, whereas that of 1600 cm<sup>-1</sup> did not move. This shows that lignin does not have a load-bearing role in the material.

A cellulose fibre prepared by dissolving a liquid crystalline of cellulose (7.5% (w/w)) in phosphoric acid to form an anisotropic solution was deformed in tension, and the peaks at 895, 1095, 1260 and 1414 cm<sup>-1</sup> were monitored for Raman band shift [7]. All peaks were observed to have shifted linearly towards lower wavenumber. However, the peak at 1414 cm<sup>-1</sup> showed the highest shift rate. Hydrogen bonding within the structure was thought to have played a significant role in the stress transfer between the adjacent cellulose chains.

Spruce latewood fibres were investigated [8]. Two peaks at 1097 and  $1602 \text{ cm}^{-1}$  corresponding to the C–C stretching of cellulose and aryl stretching of lignin were monitored. The Raman band located at  $1097 \text{ cm}^{-1}$  shifted to a lower wavenumber and was found to have returned to its original position after failure, an indication of the elastic nature of the fibre. The peak at  $1602 \text{ cm}^{-1}$  did not shift after tensile deformation was applied. Again, lignin properties in spruce latewood fibres show that it is non-load bearing. An overall shift of  $-6.5 \text{ cm}^{-1}$  and a shift rate of  $-6.1 \text{ cm}^{-1}/\text{GPa}$  for  $1097 \text{ cm}^{-1}$  Raman band were observed.

Quero et al. [9] used glyoxalisation to cross-link cellulose chain of bacterial cellulose (BC). The influence of this treatment on molecular deformation was investigated. Higher stress transfer efficiency was observed for the glyoxalisation. Treated BC network compared with unmodified samples indicating that cross-linking has taken place. The gradients of the linear fits were  $-0.9\pm0.1$  and  $-1.7\pm0.1$  cm<sup>-1</sup> for the unmodified and modified BC networks, respectively.

Following the successful application of Raman spectroscopy to monitor deformation of cellulose fibres, the application has equally received attention for cellulose-based composites. The aim was to understand the interfacial behaviour between the matrix and reinforcement phases, thereby determining the efficiency of the stress transfer of this filler at different filler weight or volume fractions.

Cotton nanowhiskers were prepared by sulphuric and hydrochloric acid hydrolysis, while tunicate nanowhiskers were developed by sulphuric acid hydrolysis [10]. Zero point seven per cent (0.7%)

volume fraction of all cellulose nanowhiskers were embedded into epoxy resin. Irrespective of the preparation method, cotton cellulose whisker had an aspect ratio (length/width) of  $\sim 19$ , while tunicate nanowhiskers had  $\sim 76$ . The Raman band initially located at  $1095~\rm cm^{-1}$  was observed for all composites. The Raman band for tunicate/epoxy and cotton/epoxy prepared by sulphuric acid shifted towards a lower wavenumber during the tensile deformation giving a shift rate of  $-2.5~\rm and -0.9~\rm cm^{-1}/\%$ , respectively. Atomic force microscopy (AFM) images reveal aggregations in the composites of cotton nanowhiskers produced by hydrochloric acid hydrolysis. This may have affected the efficiency of stress transfer.

Quero et al. [11] used Raman spectroscopy to study the stress transfer in bacterial cellulose (BC)/poly(L-lactic acid) composites. BC network with two different culturing times (3 and 6 days) was incorporated into poly(L-lactic acid). When compared with the pure BC network, the Raman bands for the composites at the two different culturing times shifted and were higher for the Raman band initially located at 1095 cm<sup>-1</sup>, indicating the stress transfer efficiency in these composites. The specific Young's moduli (Young's modulus divided by density) for both networks were the same.

Chitin is a naturally occurring renewable and biodegradable polysaccharide. It is mechanically stable, non-toxic and physiologically inert polymer. It is the second most abundant natural polymer after cellulose. There is no reported literature using Raman spectroscopy to monitor the deformation of chitin, and therefore, this work is aim at reporting the first attempt. The interest in chitin is based on the structural similarity between chitin and cellulose. Chemical chitin is identical to cellulose but for the secondary hydroxyl on the alpha carbon atom (C-2) of the cellulose molecule which is substituted with an acetamide group. The removal of acetyl group in the alpha carbon atom results into the formation of chitosan a derivative of chitin. PAA a highly amorphous polymer was chosen to investigate the effect of amorphous content on the shift of Raman peak when subjected to tensile deformation.



# Experimental methodology

Chitin Shrimp, poly(acrylic acid) and all chemicals were purchased from Sigma-Aldrich, UK. Preparation of chitin whiskers (CHW), chitin film and chitin whiskers-reinforced poly(acrylic acid) (PAA) films was carried out as reported elsewhere [12–14]. Dried chitin was mixed with 3 N HCl at a ratio of 1:30 g/ ml. The mixture is heated at 120 °C for 6 h. The suspension was diluted with distilled water, followed by centrifugation at 8000 rpm for 10 min. This process is repeated three times. Between 50 and 60 ml of suspension was transferred to a dialysis bag. The dialysis bag in a beaker was dialysed in running water for 2 h, after which in distilled water overnight. The dialysis continued for 2 more days while changing the distilled water every day. The pH level of the suspension was adjusted to 3 by adding few drops of HCl acid. The dispersion of chitin whiskers was completed by sonification. The solid content of the chitin whiskers suspension was approximately 0.3 wt%. Purified chitin was roughly crushed with domestic blender. The crushed chitin was vacuum sieved using a porcelain Buchner filter funnel having an approximate pore of 1.4 mm. The sieve chitin was dispersed in water to make 0.5 wt% nanofibre content. The pH value was adjusted to 3 by adding few drops of acetic acid. The solution was magnetically stirred over night at room temperature. The suspension was vacuum-filtered. The obtained chitin nanofibre was hot pressed for up to 60 min at a temperature of between 80 and 90 °C to form chitin film. Chitin whiskers suspension and 1 wt% PAA solution were gently mixed in beaker and magnetically stirred at room temperature for about 3-5 min adjusting the pH (which remains at 2 for all samples). The final volume for each solution is maintained at 50 ml. The solution was cast in a plastic Petri dish and allowed to dry at the fume hood for 72 h. The films were later dried in an oven at a temperature of 30 °C to remove residual water for 10 h or until the film detached itself from the dish. All films were kept in seal bags until when needed.

Deformation of chitin and its composites were investigated using Raman spectroscopy. A Renishaw system 1000 Raman imaging microscope with a low-power (25 mW) near-infrared 785-nm laser was used to record spectra from chitin whiskers and its nanocomposites. A  $50 \times 0$  objective lens was used to focus the laser on the samples to a spot size of

 $\sim 1-2 \,\mu m$ . Spectra were recorded in the range 1580–1700 cm<sup>-1</sup>, including an intense peak located at  $\sim 1622 \text{ cm}^{-1}$ . All spectra were recorded using an exposure time of 10 s with four accumulations. The laser polarisation direction was set parallel to the deformation axis of the samples. The samples were secured on a customised deformation rig (MICROT-EST 2000 module) incorporating a load cell of 2 kN (Fig. 1b). The gauge length was 20 mm, while the loading speed was 0.05 mm/min. Each sample was secured to a cardboard window specimen mount (Fig. 1a), which was clamped between the jaws of the rig. Tensile increments of 0.1% were applied to the sample. At each increment, a Raman spectrum was recorded. The strain was obtained from the displacement of the mobile grips. By curve fitting using an automated algorithm, and a mixed Gaussian-Lorentzian function, based on the work of Marquardt [15], each spectrum was fitted to find the peak positions. Chitin film and three different weight fractions of chitin (0.73, 0.41 and 0.23) were monitored for deformation. The orientation of fibrils within a composite film was measured by rotating the samples at 5° angular increments from 0° up to 360°. The intensity of the Raman peak located at  $\sim 1622 \text{ cm}^{-1}$ 

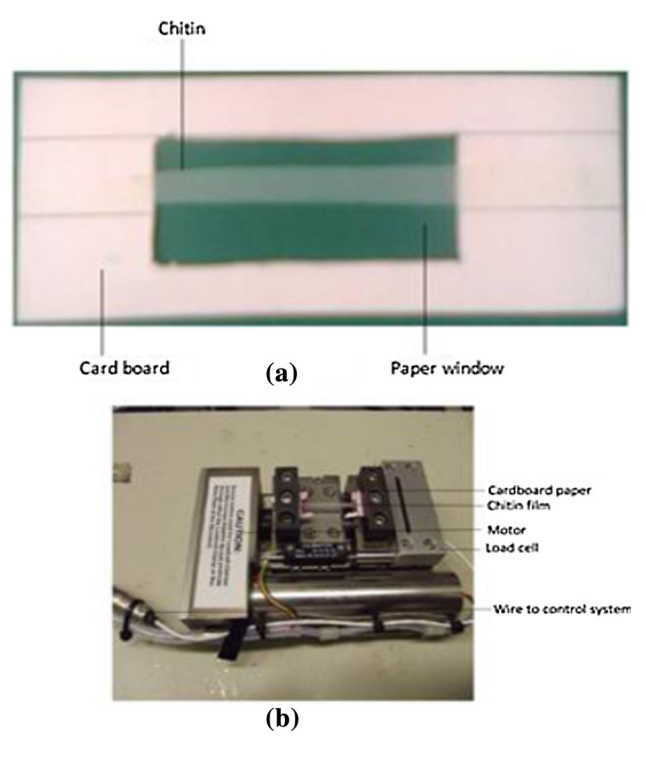


**Figure 1** a Illustration of the mechanical test sample of chitin, PAA or composite film, **b** a 2-kN load cell customised DEBEN deformation rig used to deform chitin film and CHW composites.



1.0

was recorded at each rotation increment. The films were conditioned at  $23 \pm 3$  °C,  $50 \pm 5$  RH for 48 h before deformation. An average of between 4 and 6 samples were taken for each composite. A FEG-SEM XL-30 scanning electron microscope operating at a voltage of 10 kV was used to obtain the fractured surfaces of films. JEOL-200FX transmission electron microscopy (TEM) working at an accelerating voltage of 120 kV and ImageJ software were used to get the morphology and dimensions of CHWs (length and width), respectively.

#### Results and discussion

# Morphological properties of CHWs

The TEM image of CHWs is presented in Fig. 2a. The whiskers exhibited a colloidal behaviour which is attributed to the presence of positive charge on the whisker surface due to the protonation of amino groups of chitin in an acidic form [16]. The whiskers contained chitin fragment which is slender and rodlike with sharp points. The length of the whisker is between 62 and 428 nm, and the width is 6 and 49 nm. All dimensions are broadly distributed. An ImageI analysis carried out shows that the mean length and width are  $233 \pm 92$  and  $25 \pm 11$  nm, respectively. The mean aspect ratio (L/D; L) is the length and D the diameter) is  $\approx 9.4 \pm 8.2$  nm, while the modal aspect ratio is  $\approx 10 \pm 2$  nm. This value is smaller than the earlier reported result [14], but agrees with other reports [16–18].

To confirm whether the shift of the Raman band initially located at  $\sim 1622 \text{ cm}^{-1}$  to a lower wave number, as presented in Fig. 5, is due to deformation, or caused by scattering in the data, statistical measurements were carried out on the chitin films and its composites. At the end of each strain deformation, 30 measurements at a fixed (spot size of  $\sim 1-2 \mu m$ where the laser beam was focused) position were taken; the data are presented as a histogram in Fig. 2b. The figure shows a significant shift towards a lower wavenumber. The deviations standard obtained are 0.62, 0.55, 0.63 and 0.54 for 100% (chitin film), 73, 42 and 23% CHW content, respectively.

Figure 3 shows the fractured surfaces of CHWs-reinforced composites at different loading of CHWs. From the blend films of 23, 41 and 73%, there is a clear evidence of incorporation of whiskers in the

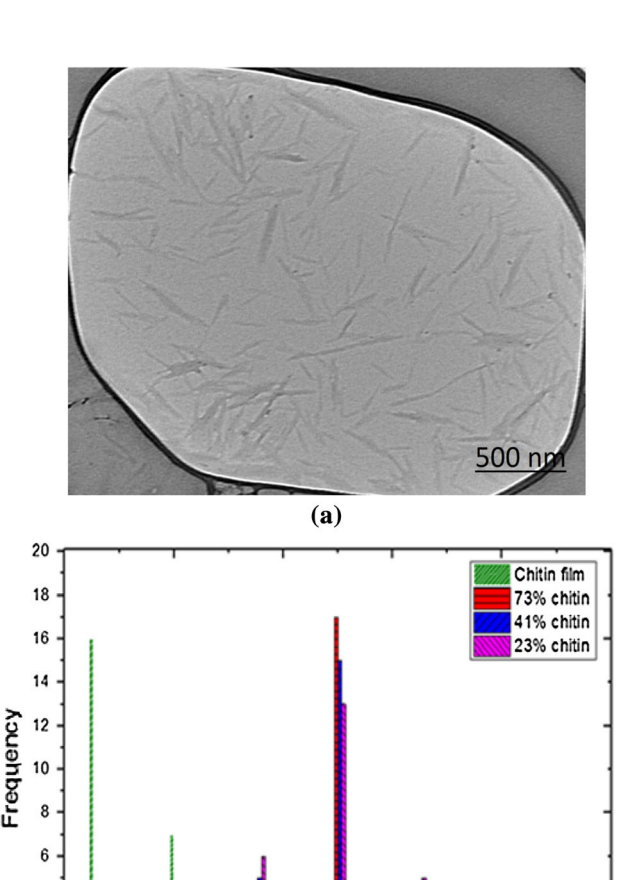


**Figure 2** TEM images of CHWs (a) and histogram distributions of 30 point measurements of CHW and its composite at the Raman band initially located at 1622 cm<sup>-1</sup>. Data were collected at a fixed spot position at different levels of tensile deformation (b).

Raman band shift (cm-1)

**(b)** 

-1.0

4

-2.0

-1.5

PAA. Regardless of the chitin content, all blend consist of randomly aligned standing fibre films. PAA fractured surface (not presented here) shows homogenous smooth cross-section devoid of lamellar layers, while fractured chitin surface shows rough and thick surface morphology. The relative smoothness of PAA fractured surface gradually disappears to a lamellar surface as the chitin content increases. The composites micrographs show the appearance of some none-uniformity voids (groves) at 41 and 23% chitin which tend to disappear at 73% chitin and none in chitin film. This is an indication of detached filler from the matrix. This can only happen when there is poor wetting between the filler and matrix. The SEM monographs for higher fillers show high degree of



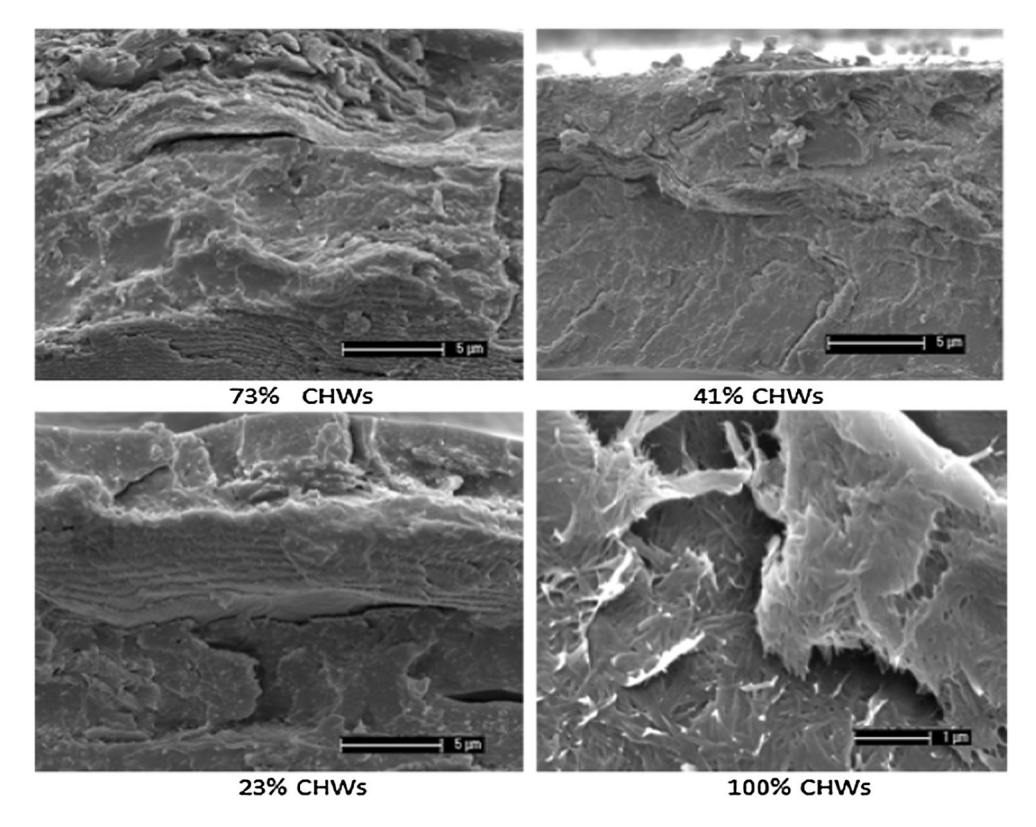


Figure 3 Fractured surfaces of CHWs reinforced PAA at different loadings of CHWs.

fibril with plastic deformations an indication of ductile failure.

#### Raman shift due to tensile deformation

Raman spectroscopy has been used to monitor stress transfer between cellulose whiskers and polymer matrices. In no previous studies has Raman spectroscopy been used to monitor chitin or its composites. Different polarisation configurations of Raman spectroscopy can be used to monitor deformation. The frequently used polarisation configurations are the parallel-parallel polarised configuration (VV) and crossed-polarised configuration (VH) [19, 20]. Rusli [20] observed that the Raman signal depends on these configurations and the maximum intensity is obtained when the polarisation direction is parallel to oriented sample axis, i.e., the parallel-parallel polarised configuration (VV). This is the configuration used to monitor the deformation of chitin film and CHW/PAA composites.

The single and double H-bonded spectrum was split into two at 1622 and 1656 cm<sup>-1</sup>. The double spectrums form the basis of amide I band for  $\alpha$ -chitin whisker [21, 22] (Fig. 4a). The Raman peak at

1622 cm<sup>-1</sup> which corresponds to the single H-bonded amide 1 spectrum was monitored during deformation. From Fig. 4a, b, it can be seen clearly that the Raman spectra have a band located at 1622 cm<sup>-1</sup>. The intensity of this band decreases with decreasing CHW content or increase in PAA. These could be attributed to the amorphous nature of PAA. For accurate determination of the peak, it is important that the intensity of the peak is high. Therefore, only filler loading of 73, 41 and 23% chitin was monitored, while those of 11 and 3% were discarded.

By curve fitting using the Lorentz/Gaussian function, the 1622 cm<sup>-1</sup> Raman peak position was obtained and the result and data are presented in Fig. 5. A band (shown as gradient) shift rate of – 1.85 cm<sup>-1</sup>/% was achieved for chitin film. This value, although from a different Raman peak position, was higher than those obtained by Pullawan et al. [23] (– 0.3 cm<sup>-1</sup>/%) for LiCl/DMAc cellulose nanocomposites, Rusli et al. [10] (0.9 cm<sup>-1</sup>/%) for epoxy/cotton cellulose nanowhiskers prepared by sulphuric acid, Rusli [24] (0.4 cm<sup>-1</sup>/%) for tunicate whiskers films produced by solution casting, and Hsieh et al. [25] (1.77 cm<sup>-1</sup>/%) for a bacterial cellulose. The obtained value here is equally less than that



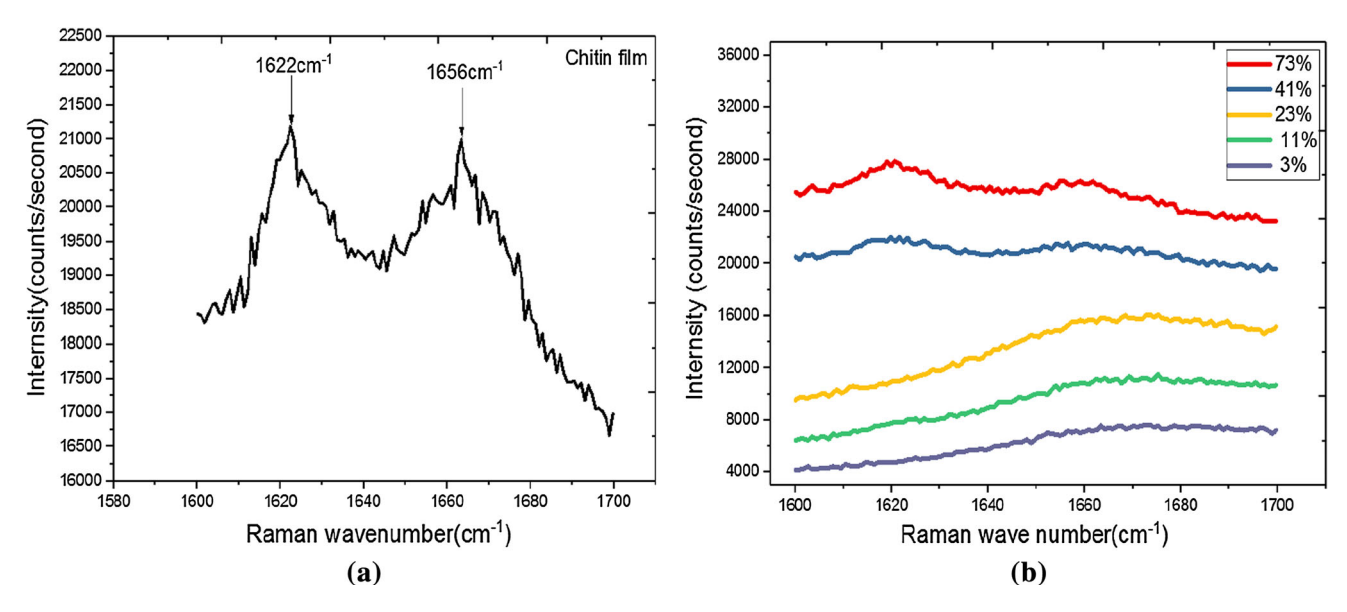
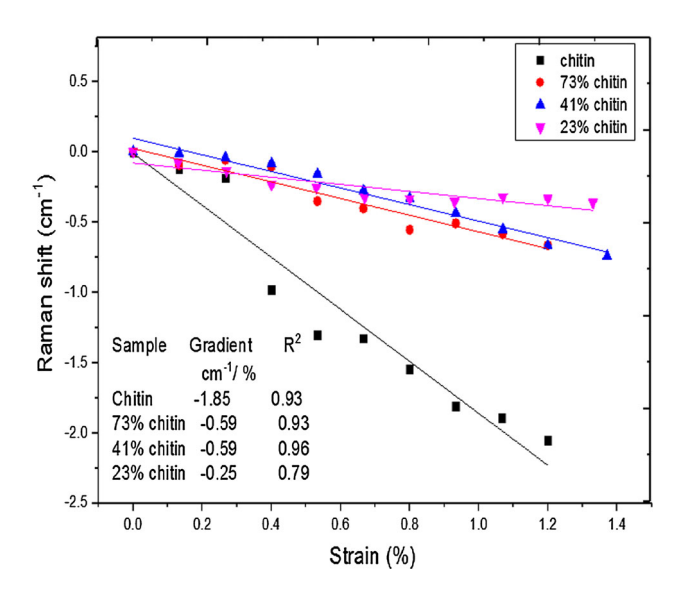


Figure 4 Raman spectra for chitin film (a) and Raman spectra for 73, 41, 23, 11 and 3% chitin before deformation (b).



**Figure 5** Raman band located at 1622 cm<sup>-1</sup> as a function of tensile strain for chitin film, 73, 41 and 23% composites.

obtained by Šturcová et al. [26]  $(-2.4 \text{ cm}^{-1}/\%)$  for a tunicate cellulose whiskers. The difference in wavenumber shift rate could be attributed to morphology, chemical and microstructures of the materials [26] and the aspect ratio of the whisker [20].

The high Raman band shift for pure chitin compared with cellulose from different sources could equally be attributed to high crystallinity of chitin as was discussed elsewhere [27] where the index of crystallinity is 0.92. The high crystallinity index (CI) is an indication that the chitin film is free from the amorphous influence [26]. From Fig. 6a at 1.2%

strain, the 1622 cm<sup>-1</sup> peak did not show any broadness, indicating the low level of amorphous in the chitin film and therefore no stress transfer between the crystalline and amorphous domains. Eichhorn et al. [28] reported that the Raman band shift of 1095 cm<sup>-1</sup> peak for cellulose II fibres is a function of both the amorphous and crystalline fractions of the polymer. It follows therefore that the high Raman band shift recorded here could be attributed to the high crystalline index of chitin. Figure 6b-d shows the band shift for CHW/PAA composites. The band shift for 73 and 41% remained at  $-0.59 \text{ cm}^{-1}/\%$ , while that of 23% was observed to be  $-0.25 \text{ cm}^{-1}/\%$ . The decrease in Raman band shift rate as the CHW content increases indicates that stress transfer is reduced on the addition of PAA a highly amorphous polymer. It also shows that efficient stress transfer can only be achieved at a higher weight or content of CHW. The reduction in stress transfer could also be attributed to a decrease in the crystallinity of the chitin fibrils on the addition of PAA. Although the dispersion of chitin was good, small aggregation of chitin fibrils within the matrix could have prevented effective reinforcement. The downward regression values for CHWs/PAA further confirm (Fig. 5) that at lower CHWs the Raman intensity is low and it will be difficult to monitor the shift rate. Similar trends have been observed elsewhere [10, 29]. Figure 6 shows the curve shifts (1622 cm<sup>-1</sup> Raman peak) in the Raman spectra for (A) chitin film, (B) 73%, (C) 41% and (D) 23% before and after deformation.



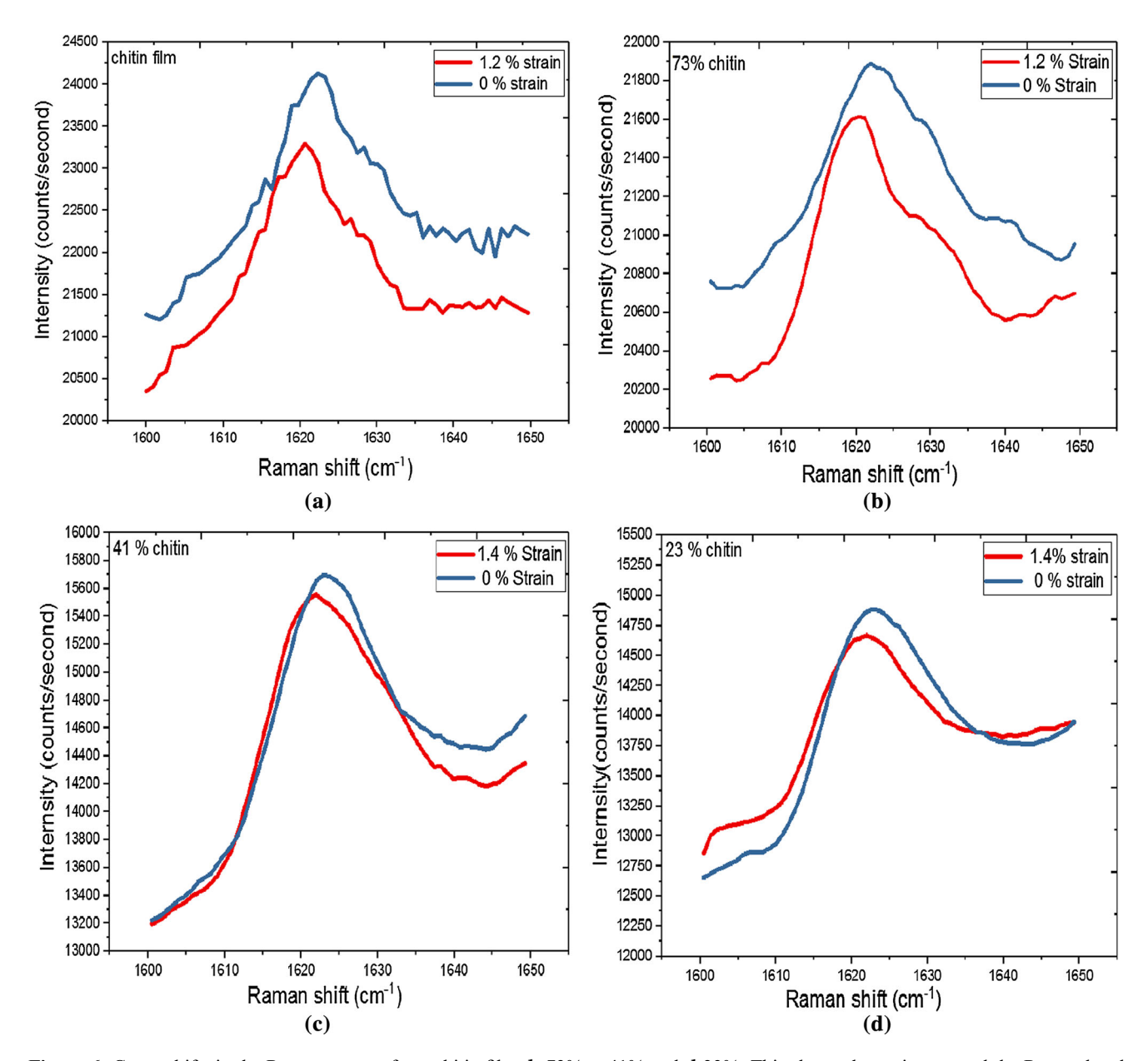


**Figure 6** Curve shifts in the Raman spectra for **a** chitin film, **b** 73%, **c** 41% and **d** 23%. This shows the region around the Raman band located at 1622 cm<sup>-1</sup> at 0% strain (black) before and 1.2 or 1.4% strain (red) after deformation.

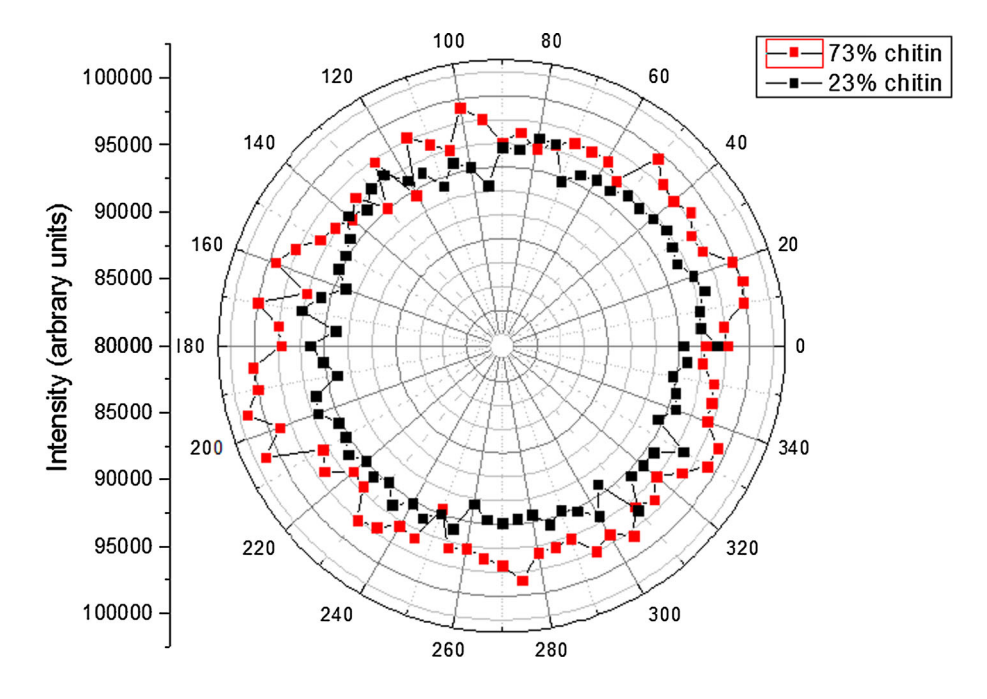
As CHWs decrease the broader the peak even at 0% strain, this is an indication of the amorphous presence in the composite, which contributes to a lower stress transfer as was discussed above.

The alignment of CHW within the PAA was also investigated. Various studies [20, 30, 31] have shown that for a cellulose whisker composite, the intensity of the Raman band located at 1095 cm<sup>-1</sup> remains relatively constant with the rotation of angle for a randomly distributed cellulose whiskers. With this in mind, the intensity of the Raman band for CHW

located at 1622 cm<sup>-1</sup> was taken at 0% strain, while the polarisation axis was set at 0°. From Fig. 7, it seems the intensity of the band located at 1622 cm<sup>-1</sup> remains the same at 0% strain indicating that CHW within PAA matrix does not have any preferential alignment confirming the random orientation of the whiskers.



Figure 7 Intensity of the Raman band located at 1622 cm<sup>-1</sup> for 73 and 23% films as a function of the angle of the specimen with respect to the polarisation axis at 0% strain.



# Determination of a single CHW modulus

In order to obtain the modulus of a single cellulose whisker, Eichhorn et al. [6] established a relationship between the gradient of the Raman band shift initially located at 1095 cm<sup>-1</sup> and the modulus. The equation is given as;

$$\frac{\mathrm{d}v}{\mathrm{d}\varepsilon} = K_{\varepsilon} E_{\mathrm{w}} \tag{1}$$

where  $K_{\varepsilon}$  is constant of proportionality and  $\frac{dv}{d\varepsilon}$  is the strain rate, and  $E_{\rm w}$  is the modulus of a single cellulose whisker. This equation applies to polymer fibres subjected to deformation. For the equation to be valid, it was assumed that the cellulose whisker had a uniform stress in both amorphous and crystalline regions. A value of  $-4.3 \text{ cm}^{-1}/\text{GPa}$  was established for cellulose whiskers [6]. Substituting the band shift rate  $(-1.85, 0.59, 0.59, -0.25 \text{ cm}^{-1}/\%, \text{ and}$  $-4.3~{\rm cm}^{-1}/{\rm GPa}$  for  $K_{\epsilon}$  value) for chitin film, 73, 41 and 23% into Eq. 1,  $E_{\rm w}$  the modulus obtained for chitin films 73, 41 and 23% is 43, 14, 14 and 5.8 GPa, respectively. The values obtained above are for a random network of whiskers. Therefore, to calculate the true modulus  $E_{w}^{t}$  an efficiency factor  $\eta_{o}$  as related to Eq. 2 is used [10].

$$E_{\mathbf{w}}^t = \eta_o^{-1} E_{\mathbf{w}} \tag{2}$$

The distribution of chitin orientations could be two (2D) or three-dimensional (3D) random. The

efficiency factor for a two in-plane random network of fibres for various angles of the deformation fibres has been outlined [32]. Using the integral of Eq. 3 and substituting the values into Eq. 2, the real modulus for chitin and reinforced composites with cellulose and cellulose-reinforced composites from the literature are presented in Table 1.

$$\eta_o = \frac{1}{\pi} \int_{-\frac{x}{4}}^{\frac{x}{2}} \cos^4 \theta d\theta = \frac{3}{8}$$
(3)

Although the strain rate was measured at the Raman peak position of 1095 cm<sup>-1</sup> for cellulose, Table 1 shows that cellulose fibres give varying values of

**Table 1** The actual modulus of chitin film, different cellulose whiskers, CHW and cellulose-reinforced composites for a 2D network of fibres

Sample	$E_{\rm w}^t$ (GPa)	References
Chitin film	115	This work
Bacterial cellulose	79–88	[30]
Bacterial cellulose	114	[25]
Tunicate whiskers	143	[26]
73% CHWs	37	This work
41% CHWs	37	This work
23% CHWs	16	This work
Cotton cellulose/epoxy	58	[20]
Tunicate whiskers/epoxy	155	[20]
Microfabricated cellulose	29–36	[31]



modulus and the same with cellulose-reinforced composites. The reasons for the variations could be attributed to the source of the bacterial cellulose, the level of crystallinity and the effectiveness of the matrix to transfer stress to the fibre. At higher crystallinity, the influence of amorphous phase is reduced [26]. The variation could also be attributed to the differences in aspect ratio, as this will affect the stress transfer. The low values obtained for 73, 41 and 23% compared with those of cellulose-reinforced composites indicate the presence of an amorphous influence and not the selected Raman peak. This is confirmed by the broadening of the peak at 1622 cm<sup>-1</sup> as filler reduces.

## **Conclusions**

CHWs was produced by acid hydrolysis and reinforced with poly(acrylic acid). Raman Spectroscopy has shown in the literature can be used as a tool for the estimation of the Young modulus of microcrystalline cellulose. This device has been used for the first time to estimate the Young modulus of CHW film and CHWs reinforced composite. CHW within PAA matrix monitored by Raman spectroscopy shows that the whiskers do not have preferential alignment. The Raman band located at 1622 cm<sup>-1</sup> was observed to have shifted to a lower waveband when Raman was used in monitoring the deformation. A Raman band rate of  $-1.85 \text{ cm}^{-1}/\%$  was attained for chitin film. These values decrease as filler content decreases, an indication that the Raman shift can be achieved at a low level of amorphous material. The results obtained here are comparable with those in the literature obtained from cellulose nanowhiskers and cellulose-reinforced composites. The differences in outcome could be attributed to among other things on the aspect ratio and the level of crystallinity.

# Compliance with ethical standards

**Conflict of interest** The author declares that he has no conflict of interest.

## References

[1] Bauer NJ, Wicksted JP, Jongsma FH, March WF, Hendrikse F, Motamedi M (1998) Noninvasive assessment of the

- hydration gradient across the cornea using confocal Raman spectroscopy. Invest Ophthalmol Vis Sci 39:831–835
- [2] Wang C, Vickers TJ, Mann CK (1997) Direct assay and shelf-life monitoring of aspirin tablets using Raman spectroscopy. J Pharm Biomed Anal 16:87–94
- [3] Wartewig S, Neubert RH (2005) Pharmaceutical applications of mid-IR and Raman spectroscopy. Adv Drug Deliv Rev 57:1144–1170
- [4] Brunner E, Ehrlich H, Schupp P et al (2009) Chitin-based scaffolds are an integral part of the skeleton of the marine demosponge *Ianthella basta*. J Struct Biol 168:539–547
- [5] Ehrlich H, Maldonado M, Spindler K et al (2007) First evidence of chitin as a component of the skeletal fibres of marine sponges. Part I. Verongidae (Demospongia: Porifera). J Exp Zool (Mol Dev Evol) 308b:347–356
- [6] Eichhorn SJ, Sirichaisit J, Young RJ (2001) Deformation mechanisms in cellulose fibres, paper and wood. J Mater Sci 36:3129–3135. https://doi.org/10.1023/A:1017969916020
- [7] Eichhorn SJ, Young RJ, Davies RJ, Riekel C (2003) Characterisation of microstructure and deformation of high modulus cellulose fibres. Polymer 44:5901–5908
- [8] Gierlinger N, Schwanninger M, Reinecke A, Burgert I (2006) Molecular changes during tensile deformation of single wood fibres followed by Raman microscopy. Biomacromolecules 7:2077–2081
- [9] Quero F, Nogi M, Lee K et al (2011) Cross-linked bacterial cellulose networks using glyoxalization. Appl Mater Interfaces 3:3490–3499
- [10] Rusli R, Shanmuganathan K, Rowan SJ, Weder C, Eichhorn SJ (2011) Stress transfer in cellulose nanowhisker composites-Influence of whisker aspect ratio and surface charge. Biomacromolecules 12:1363–1369
- [11] Quero F, Nogi M, Yano H et al (2010) Optimization of the mechanical performance of bacterial cellulose/poly(L-lactic) acid composites. Appl Mater Interfaces 2:321–330
- [12] Junkasem J, Rujiravanit R, Supaphol P (2006) Fabrication of α-chitin whisker-reinforced poly (vinyl alcohol) nanocomposite nanofibers by electrospinning. Nanotechnology 17:4519–4528
- [13] Junkasem J, Rujiravanit R, Grady BP, Supaphol P (2010) X-ray diffraction and dynamic mechanical analyses of αchitin whisker-reinforced poly (vinyl alcohol) nanocomposite nanofibers. Polym Int 59:85–91
- [14] Morin A, Dufresne A (2002) Nanocomposites of chitin whiskers from Riftia tubes and Poly(caprolactone). Macromolecules 35:2190–2199
- [15] Marquardt DW (1963) An algorithm for least-square estimation of nonlinear parametrics. Soc Ind Appl Math 11:431–441



- [16] Marchessault RH, Morehead RR, Walter NM (1959) Liquid crystal systems from fibrillar polysaccharides. Nature 184:632–633
- [17] Lu Y, Weng L, Zhang L (2004) Morphology and properties of soy protein isolate thermoplastics reinforced with chitin whiskers. Biomacromolecules 5:1046–1051
- [18] Sriupayo J, Supaphol P, Blackwell J, Rujiravanit R (2005) Preparation and characterization of α-chitin whisker-reinforced poly(vinyl alcohol) nanocomposite films with or without heat treatment. Polymer 46:5637–5644
- [19] Deng L, Eichhorn SJ, Kao CC, Young RJ (2011) The effective Young's modulus of carbon nanotubes in composites. Appl Mater Interfaces 3:433–440
- [20] Rusli R (2011) Interfacial micromechanics of natural cellulose whisker polymer nanocomposites using Raman spectroscopy, Ph.D. Dissertation, The University of Manchester, School of Materials
- [21] Cárdenas G, Cabrera G, Taboada E, Miranda SP (2004) Chitin characterization by SEM, FTIR, XRD, and 13C cross polarization/mass angle spinning NMR. J Appl Polym Sci 93:1876–1885
- [22] Bo M, Bavestrello G, Kurek D et al (2012) Isolation and identification of chitin in the black coral *Parantipathes larix* (Anthozoa: Cnidaria). Int J Biol Macromol 51:129–137
- [23] Pullawan T, Wilkinson AN, Zhang LN, Eichhorn SJ (2014) Deformation micromechanics of all-cellulose nanocomposites: comparing matrix and reinforcing components. Carbohydr Polym 100:31–39
- [24] Rusli R, Shanmuganathan K, Rowan SJ, Weder C, Eichhorn SJ (2010) Stress transfer in anisotropic and environmentally

- adaptive cellulose whisker nanocomposites. Biomacro-molecules 11:762–768
- [25] Hsieh Y-C, Yano H, Nogi M, Eichhorn SJ (2008) An estimation of the Young's modulus of bacterial cellulose filaments. Cellulose 15:507–513
- [26] Šturcová A, Davies GR, Eichhorn SJ (2005) Elastic modulus and stress-transfer properties of tunicate cellulose whiskers. Biomacromolecules 6:1055–1061
- [27] Ofem MI (2015) Properties of chitin whisker reinforced poly(acrylic acid) composites, Ph.D. Dissertation. The University of Manchester, School of Materials
- [28] Eichhorn SJ, Young RJ, Davies GR (2005) Modeling crystal and molecular deformation in regenerated cellulose fibres. Biomacromolecules 6:507–513
- [29] Pullawan T, Wilkinson AN, Eichhorn SJ (2012) Influence of magnetic field alignment of cellulose whiskers on the mechanics of all-cellulose nanocomposites. Biomacromolecules 13:2528–2536
- [30] Quero F (2011) Interfacial micromechanics of bacterial cellulose bio-composites using Raman spectroscopy, Ph.D. Dissertation. The University of Manchester, School of Materials
- [31] Tanpichai S, Quero F, Nogi M, Yano H, Young RJ, Lindström T, Sampson WW, Eichhorn SJ (2012) Effective Young's modulus of bacterial and microfibrillated cellulose fibrils in fibrous networks. Biomacromolecules 13:1340–1349
- [32] Eichhorn SJ, Young RJ (2001) The Young's modulus of microcrystalline cellulose. Cellulose 8:197–207

